Diagnosis of incipient electrical defects on long cables using a chaotic Duffing oscillator

Fabrice Auzanneau

Diagnosis of incipient electrical defects on long cables using a chaotic Duffing oscillator

Fabrice Auzanneau

***Abstract*— Electrical wires are always present in critical modern systems, for the transmission of energy and signals. Due to ageing or harsh environmental conditions, cables can develop defects that can reduce their performance and create severe problems. Reflectometry-based methods have been studied and implemented over the last thirty years and have shown good performance in detecting faults in cable networks. They rely on the analysis of echoes created by faults on the cable, and can detect defects whose echoes are a few percent of the input signal. But these methods are limited when it comes to detecting incipient faults characterized by echoes one order of magnitude smaller.**

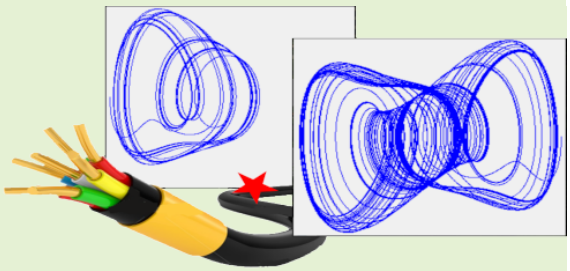

This paper presents the proof of concept of an entirely different diagnosis method. The method proposed here does not analyse the signal returned by the cable but uses this signal to disturb a system in an unstable equilibrium position. A chaotic Duffing oscillator is coupled to the cable under test and a test signal is sent into the cable: the returned signal is added to the oscillator control signal. The system parameters are chosen so that the oscillator is at the limit of stability, and a very slight disturbance of the cable causes a change in behavior that is much easier to detect than a very small peak sometimes drowned in noise on a reflectogram.

The sensitivity of this new method is higher than that of state-of-the-art ones, enabling it to detect faults of signature of 1 percent or less of the amplitude of the test signal in long cables.

***Index Terms*— Cable, Chaos, Chaotic oscillator, Fault diagnosis, Virtual sensor.**

I. Introduction

ELECTRICAL wires are used in almost all modern application domains, both public and industrial, for power and signal transmission [1]. They are considered as the backbones of electrical installations, which heavily depend on their service and reliability. In the transport sector, modern cars carry more than 5 km of cables in cumulative length, and their importance has grown with the advent of the electric vehicle. In aviation, the length of cables has increased steadily since the end of the 20th century, and regulation authorities and aircraft manufacturers have become aware of their importance [2] following two tragic accidents in the late 1990s. The concept of Electrical Wiring Interconnect System (EWIS) was created and the U.S. Federal Aviation Administration (FAA) published EWIS regulations and guidance for equipment manufacturers and aircraft makers. The EWIS is now considered a critical aircraft system on its own.

Moreover, the importance of electrical cables has also been recognized in other industrial sectors. The recent exponential growth in artificial intelligence applications has led to the construction of numerous large-scale infrastructures or computing farms hosting huge numbers of cloud servers. Depending on their size, these farms are likely to be equipped with lengths of electrical cable that can reach or exceed a thousand kilometers.

The author is with Université Paris-Saclay, CEA, List, F-91120, Palaiseau, France. (email fabrice.auzanneau@cea.fr)

These are just a few examples of the large-scale use of electrical wires, all of which demonstrate their crucial importance. Defects or failures in the wired network can have catastrophic consequences, in human, technical and economic terms. Electrical network diagnostic, which provides information on fault detection, severity and location, can be of major importance in all these application areas.

Among several diagnostic methods, reflectometry has been shown to have the highest potential [3]. As with radar, reflectometry injects an electrical probe signal at one end of the network under test. This signal propagates along the cables, and each impedance discontinuity encountered (load, junction or fault) sends part of its energy back to the injection port. The analysis of the received signal (called reflectogram) provides information on the presence, location and type of these discontinuities.

Often used in the time domain, reflectometry generates a signal made up of numerous peaks, corresponding to the various discontinuities in the network. The amplitude of these peaks can vary greatly depending on the impact of each discontinuity. In the case of a defect, a distinction is made between a hard defect (short-circuit or open circuit [4]) and a soft defect (any other defect). As shown in [5], soft defects soft faults are characterized by peaks on the reflectogram of an amplitude around a few percent of the TDR injected signal, but they can be detected if the measurement is not too noisy. The amplitude of a peak associated to a soft defect can be

very low, or even hidden in the measurement or propagation noise. Incipient defects [6], [7], defined as the precursors of soft defects, require specific detection methods, which are still being studied in laboratories. Their reflectometry signatures are an order of magnitude smaller than soft defects.

Some reflectometry methods use sine waves as probe signals (Frequency Domain Reflectometry – FDR) [8] and analyse the standing waves present on the line: they are mainly limited to hard defects.

However, as stated above, all the current diagnosis methods rely on the analysis of the measured reflectogram. Kafal et al. [9] have used Finite Element Method and a genetic algorithm to characterize the incipient defect's electrical parameters. Lee et al. [10] used Time–Frequency Domain Reflectometry (TFDR) to filter the measured signal and infer the position of the fault. Time-Reversal (TR) imaging methods [11] provide very accurate position information but have difficulties in the presence of multiple defects [12]. But all these methods require additional electronic components and complex signal processing algorithms, and sometimes a numerical model or the use of commercial numerical simulation software to provide a baseline of a fault-free cable. As a result, they cannot easily deal with propagation noise due to inhomogeneities, which create additional peaks that can be mistaken for defects, creating false alarms.

Chaos has been used recently to enhance the performances of Time Domain Reflectometry (TDR) [13]–[16], taking benefit of the possibility to generate virtually an infinite number of probe signals of arbitrary length. The use of binary chaotic signals enables the accurate detection of intermittent defects [17] and amplifies the signatures of incipient defects for better detection [18], [19]. But these methods are still based on reflectogram analysis, and are therefore limited by the sensitivity of the electronic systems they use. They can't distinguish a very weak peak too close to another peak with a higher amplitude, such as a soft defect close to a junction or connector. Furthermore, they cannot recognize the peak of a soft defect from the peak due to local propagation inhomogeneity on the cable in question.

Incipient faults are characterized in a reflectogram by very low-amplitude peaks, which are difficult to distinguish because they are often drowned in noise or hidden by other nearby peaks. But it is very important to be able to detect them as early as possible - before they develop into more serious faults, as they are linked to early cable damage (cracks in the insulation, incipient corrosion, local heating) that can be corrected by a minor maintenance operation. However, it has been shown that the intensity of TDR echoes is not a reliable estimator of fault severity [20], as faults of very different importance can generate virtually identical echoes. In this context, the usual methods of analyzing reflectograms to diagnose the condition of a cable are no longer appropriate, and it is necessary to propose alternative methods. Chaos-based weak signal detection methods have been studied for many years [21], focusing on the use of chaotic oscillators coupled to a physical system [22]. These methods are highly effective due to their noise immunity and their sensitivity to specific frequency signals.

This article presents the proof of concept of a new method that no longer relies on analysis of the measured reflectogram, but on observation of the behavior of a chaotic oscillator at the limit of stability. As with standard reflectometry methods, a test signal is injected into the cable, but the measured signal is added to the control signal of a Duffing oscillator whose parameters are chosen so that it is at the chaotic transition limit. This chaotic system is highly sensitive to disturbances, such as the signal returned by the presence of an incipient fault. Any transition to or from chaotic behavior is easily detected, indicating the appearance of a fault on the monitored cable.

The paper is organized as follows: section II provides more details on the weak signal detection methods and the chaotic oscillators used, section III presents the numerical model and section IV gives simulation results. Section V shows a possible hardware implementation and section VI concludes the paper.

II. Weak Signal Detection Using Chaotic Oscillators

A. The Duffing oscillator

The Duffing oscillator [23] is a nonlinear dynamic system which is commonly used for the detection of weak periodic signal [24], [25], defined by:

$$\frac{1}{\omega^2}\frac{d^2x}{dt^2} + \frac{\delta}{\omega}\frac{dx}{dt} - x + x^3 = \gamma\cos(\omega t) \tag{1}$$

where δ is a damping term and $\gamma cos(\omega t)$ is the driving force, which dictates the oscillation rhythm at the frequency f, with $\omega = 2\pi f$. Depending on the values of the parameters, the Duffing oscillator can have either a periodic or a chaotic behavior.

The usual way to solve equation (1) is to decompose it into a set of two first-order differential equations, as follows:

$$\begin{cases} \dfrac{dx_1}{dt} = \omega x_2 \\ \dfrac{dx_2}{dt} = \omega\left(-\delta x_2 + x_1 - x_1^3 + \gamma\cos(\omega t)\right) \end{cases} \tag{2}$$

An eighth-order Runge Kutta algorithm is used to solve system (2). Plotting x_2 as a function of x_1 in time generates a phase diagram, which emphasizes the oscillator's state: figure 1 compares the two states, chaotic on the left and periodic on the right, t varying from 0 to 2000 seconds in both cases. Depending on the initial values, the oscillator may reach the periodic state sooner.

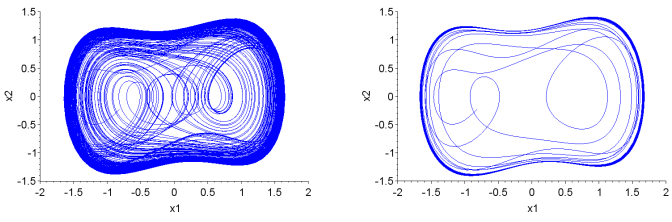

Fig. 1. Chaotic and periodic behavior examples of a Duffing oscillator.

Adding noise does not change these results [26].

B. Weak signal detection

If a perturbation signal – the weak signal to be detected – is added to equation (1), the right-end side changes as follows:

$$S(t) = \gamma\cos(\omega t) + a\cos(\omega t + \phi) \tag{3}$$

where ϕ is a phase shift and a is the amplitude of the weak signal, which is supposed very small compared to γ.

The principle of the detection method is to choose the values of γ and δ in order to put the oscillator in a critical state, very close to the chaotic transition.

Theoretical analysis has shown that when f varies, the state of the oscillator can change from periodic to chaotic. But in our case, the driving signal will be used as a reflectometry probe signal injected into the cable under test: it must remain unchanged during diagnosis and f must be constant. Therefore we choose a critical value for γ, denoted γ_c, defined as a value for which a small change will imply a state transition in the oscillator. Equation (3) can be written in a different form:

$$S(t) = \Gamma\cos(\omega t + \theta) \tag{4}$$

where

$$\Gamma = \sqrt{\gamma_c^2 + 2a\gamma_c\cos\phi + a^2} \tag{5}$$

If the amplitude of the total signal Γ is higher than a threshold value, the oscillator's state will change, and the weak signal will be detected. We speak of a 'forward transition' if the state goes from periodic to chaotic and a 'backward transition' in the other case (figure 2).

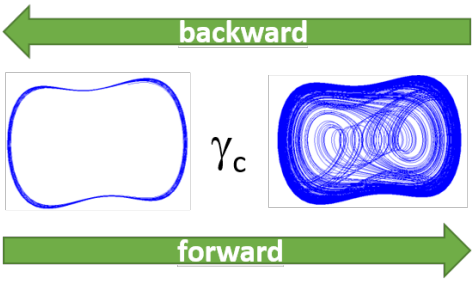

Fig. 2. Forward and backward detection.

III. Simulation Model

A. Synoptic

Figure 3 presents a first synoptic of the weak signal detector. The FDR block generates the probe signal $\gamma\cos(\omega t)$, which is the monochromatic signal also used as the driving signal of the oscillator. This signal is injected into the cable under test. Since we expect the cable to return only the signal due to the incipient fault, the cable's impedance must be matched at the input to the signal generation system, as well as at its end. This is only required for the drive frequency f.

The Duffing system is then put in the chosen state: periodic for a forward transition, or chaotic for backward. The drive signal is injected into the cable and the measured signal is added to the drive signal of the oscillator. The round trip time

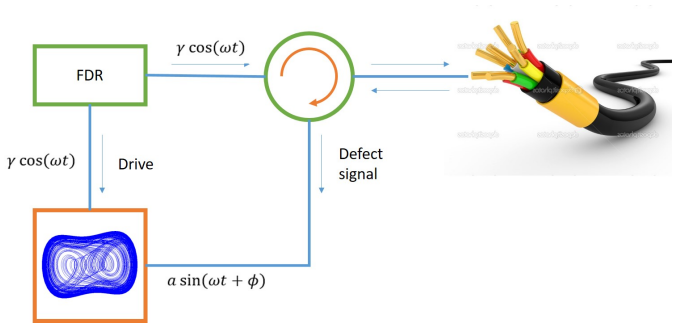

Fig. 3. Synoptic of a Duffing oscillator-based weak signal detector for cable diagnosis.

necessary for the signal to reach the defect and bounce back to the system creates a phase shift equal to:

$$\phi = 2k(\omega)d \tag{6}$$

where $k(\omega)$ is the propagation constant of the cable at the chosen frequency.

B. Transition detection

To detect a transition, it is necessary to be able to estimate whether the Duffing oscillator's behavior has changed. The Lyapunov exponents [27] are a standard measure of a system's degree of chaos. They measure the rate of divergence of two nearby points in the system's history. A chaotic system has at least one positive Lyapunov exponent, implying that it is highly sensitive to initial conditions. On the other hand, if all Lyapunov exponents are negative, the system is stable.

The most common computing techniques are the Gram-Schmidt method, which iteratively orthogonalizes the tangent vectors in the system's trajectory, and the Wolf algorithm, which calculates the time evolution of the distance between nearby trajectories to derive the Lyapunov exponents. But the calculation of Lyapunov exponents can be complex and computationally intensive.

In this application, if we compare the shapes of the trajectories of the chaotic and periodic phases of the Duffing oscillator (figure 1), it appears that the central zone is more strongly occupied by the chaotic behavior than by the periodic one. A simpler indicator would be the presence rate of the trajectory in the central zone:

$$P(N) = \frac{1}{N}\sum_{i=1}^{N} p(i),\ p(i) = \begin{cases} 1, & \text{if } ||x(i)|| < R \\ 0, & \text{otherwise} \end{cases} \tag{7}$$

where $||x(i)|| = \sqrt{x_1^2(i) + x_2^2(i)}$, and $R = 0.3$ provides a reasonably good estimator.

However, as shown later in section IV, there can be different types of transitions, which are not necessarily compatible with this estimator. We may need to use ad-hoc transition detection methods.

IV. Simulation Results

A. Finding critical states

Finding critical values of the parameters, putting the oscillator at the edge of a state transition, is a complex problem.

To find such critical values, a specific tool has been written in Python, enabling a quick search by trial and error. This tool is based on the *tkinter* library, for maximum interactivity. It plots in a graphical window the oscillator's trajectory corresponding to a pair of γ and δ parameters, and the initial values for the simulation. By pressing the arrow keys on the keyboard, one can modify the value of γ, either by adding or subtracting a quantity, or by dividing or multiplying this quantity by 2. When a change in behavior is visible in the graphical window, this means that the current γ value is close to a critical value. By dividing the quantity while remaining at the transition limit, an increasingly accurate approximation of the critical parameter can be obtained. Figure 4 plots two trajectories of the oscillator in the plane x_1, x_2 (no units) and shows an example of a critical value of γ with δ = 1. For the same set of initial values, changing γ from 0.789961073994637 to 0.7899610742926603 provides two very different trajectories.

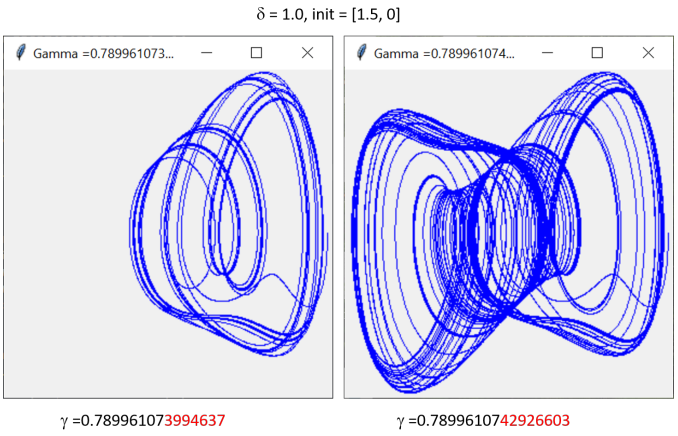

Fig. 4. Example of a critical value of γ. A difference of 2.98 10^{-10} implies the transition from a pseudo-periodic positive trajectory (left) to a bipolar chaotic trajectory (right), all other things being equal.

The transition shown on Figure 4 is categorized as "pseudo-periodic positive to bipolar chaotic". The term "positive" refers to the fact that on the left part of Figure 4, the trajectory remains on the right half of the picture, i.e. on the positive horizontal axis. Other kinds of trajectories have been identified, and will be exploited later, such as:

- bipolar pseudo-periodic,
- positive chaotic,
- bipolar chaotic.

B. Defect detection and location using chaos transition

In this chapter, Figures 5, 7, 9 and 11 compare the evolution of oscillator trajectories with and without the presence of the disturbance fault, in the x_1, x_2 (unitless) plane.

Table I summarizes the simulation settings.

We first use critical values of γ_c = 0.7899768132015731 and δ = 1, with initial values of [0.0, 0.0]. Figure 5 shows the unperturbed trajectory of the oscillator on the upper part (blue curve): this is another example of pseudo-periodic positive trajectory. If a defect on the line occurs, it changes the behaviour of the oscillator. We added a weak signal of amplitude a = 0.008 V after 2.5 10^{-7} seconds (green line on Figure 6). The trajectory changes drastically, and becomes as shown on the lower part of Figure 5 (red curve). Figure 6 shows the evolution of x_1, x_2 without (two first curves) and with (two last curves) the perturbation. Comparison of the two red curves of Figure 6 shows the forward transition from pseudo-periodic to chaotic. Note that the amplitude of the signal is very small compared to the amplitude of the oscillator, showing the detection of a very weak defect. The transition occurs near t = 3.10^{-7} seconds, 500 ns after the occurrence of the defect. Assuming a propagation velocity inside the cable of c = 2.10^8 m/s, this represents a location error of 5m.

Using γ_c = 0.619689017534256 and δ = 0.8, and initial values equal to [1.5, 0.0], leads to the transition from positive chaotic to bipolar chaotic, as shown on Figure 7. This time, the signal's amplitude is even smaller a = 0.004 V, and the transition is detected near 2.7 10^{-7} seconds (Figure 8), leading to a location error of 2m.

Using γ_c = 0.5382418727874758 and δ = 0.3 leads to the backward transition from bipolar chaotic to bipolar periodic, as shown on Figure 9. This time, the signal's amplitude is down to a = 0.001 V, and the transition is detected near 2.9 10^{-7} seconds (Figure 10), leading also to a location error of 4m. The upper plots of Figure 10 show that this choice of parameters γ and δ leads also to a maximum detection time near $t_{max} = 9.10^{-6}$ seconds, equivalent to a maximum length of cable of

$$D_{max} = \frac{t_{max} * c}{2} = 1350m$$

Using γ_c = 0.2728 and δ = 0.3 leads to the forward transition from positive pseudo-periodic to bipolar chaotic, as shown on Figure 11. This time, the signal's amplitude is down to a = 0.0008 V (0.05% of the oscillator's amplitude), and the transition is detected near 3.7 10^{-7} seconds (Figure 12), leading to a location error of 12m.

The extent of the location error obtained means that this method can currently only be applied to the diagnosis of long cables, i.e. in the range of tens of meters or longer.

C. Artificial intelligence tool for transition detection

As explained in section III-B, one can use the presence rate of the trajectory in the central zone to estimate the chaotic degree of a given trajectory. Figure 13 displays the values of $P(300)$ for the unperturbed oscillator of the first case, γ_c = 0.7899768132015731 (upper blue curve) and the oscillator after the occurrence of the defect (medium red curve). The bottom green curve plots the difference of the two aforementioned curves: it provides a simple way to detect a change in the trajectory. This is quite similar to the use of a baseline [28], i.e. a reference measurement for a healthy wired network, for comparison. A similar example is shown on Figure 14, for the third case (γ_c = 0.5382418727874758).

It is also possible to train a neural network to recognize the states of a given oscillator and raise an alarm when it detects a transition. We have defined and trained a simple 1D

Figure	δ	γ	Initial state	Final state	Defect's amplitude
5	1	0.7899768132015731	Positive pseudo-periodic	Bipolar chaotic	0.008
7	0.8	0.619689017534256	Positive chaotic	Bipolar chaotic	0.004
9	0.3	0.5382418727874758	Bipolar chaotic	Bipolar periodic	0.001
11	0.3	0.2728	Positive pseudo periodic	Bipolar chaotic	0.0008

TABLE I
SIMULATION SETTINGS

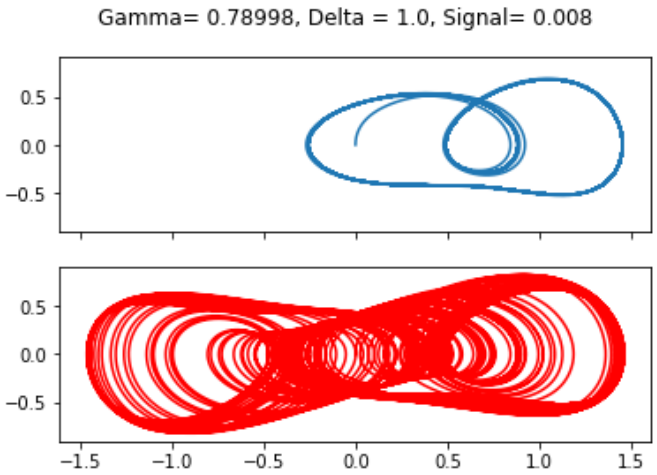

Fig. 5. Duffing oscillator trajectory without (blue) and with (red) the perturbation.

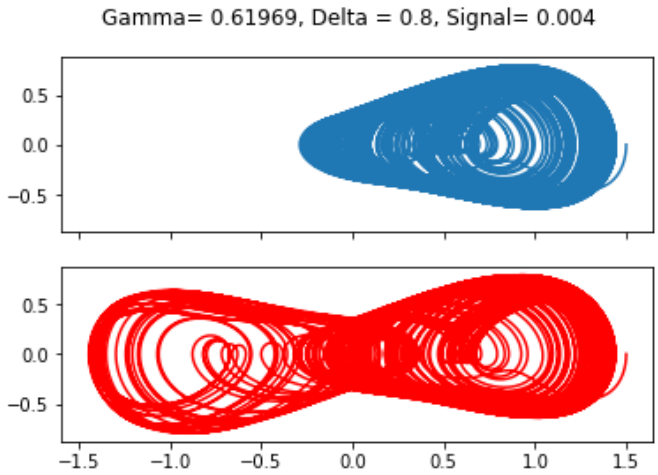

Fig. 7. Duffing oscillator trajectory without (blue) and with (red) the perturbation.

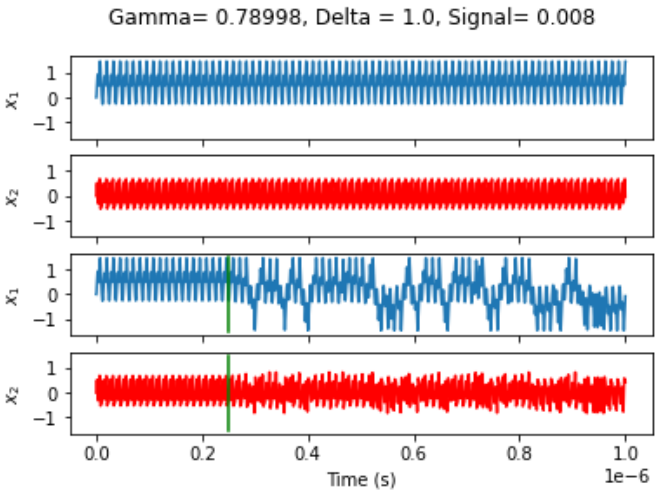

Fig. 6. Plot of the Duffing variables showing the transition from pseudo-periodic to chaotic, the defect occurs at 2.5 10^{-7}s (green line).

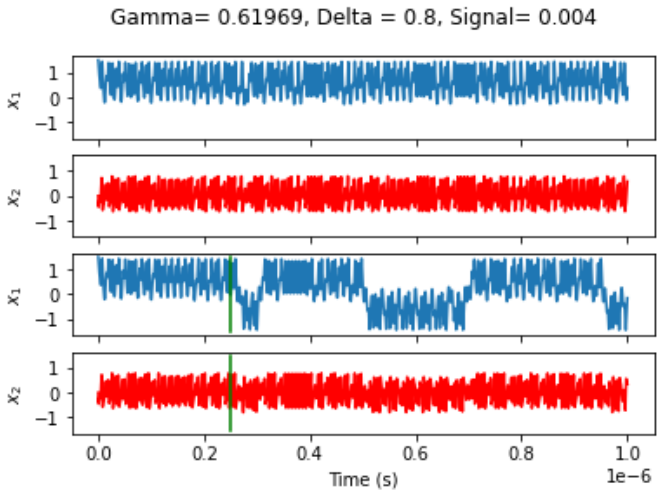

Fig. 8. Plot of the Duffing variables showing the transition from positive chaotic to bipolar chaotic, the defect occurs at 2.5 10^{-7}s (green line).

convolutional network made of 2 convolutional layers and 2 fully connected layers. Figure 15 details the network topology. The input signal is divided into 100-sample chunks which are normalized between -1 and 1 before being injected into the first 1D convolutional layer. A pooling layer calculates the maximum value of patches of the feature map and subsamples the signal for injection into two fully connected layers. All intermediate layers use ReLu (Rectified Linear Unit) activation. A SoftMax layer transforms the output of the last layer into a probability that the input vector is in one or other of the categories. The input data is an array of 100 samples of the x_2 variable over 4 periods of the oscillator's drive, and the output is either 'chaotic' or 'pseudo periodic'. The network has only 43854 trainable parameters which require 17.5 kB of memory. It was trained during 1000 epochs in less than 2 seconds, with training data generated on the fly using the oscillator shown on Figures 9 and 10, and presents a recognition rate of 97%. The network detected a change in the oscillator state at 2.75 10^{-7} s, which is more accurate than the previous method which detected the transition at 2.95 10^{-7} s (Figure 14). The location accuracy is 2.5m using the neural network, compared to 4.5m with the method based on the presence rate of the trajectory

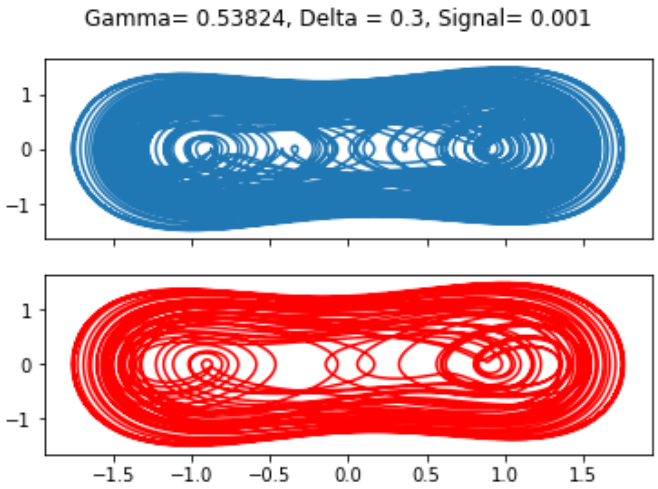

Fig. 9. Duffing oscillator trajectory without (blue) and with (red) the perturbation.

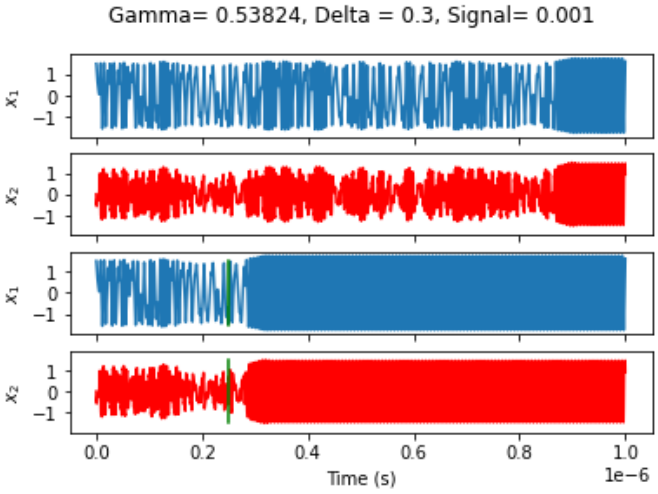

Fig. 10. Plot of the Duffing variables showing the transition from chaotic to pseudo-periodic, the defect occurs at 2.5 10^{-7}s (green line).

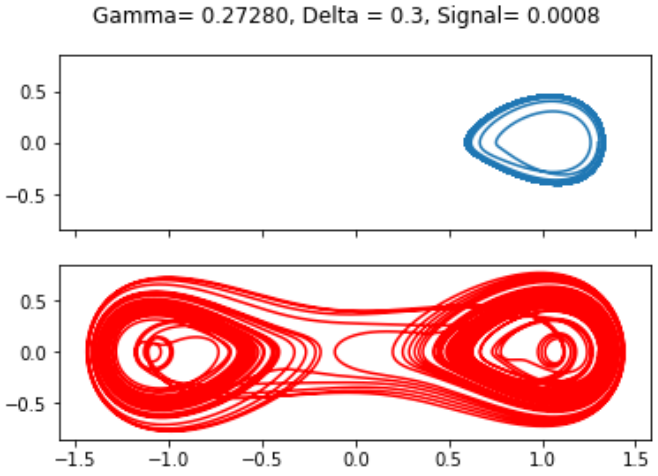

Fig. 11. Duffing oscillator trajectory without (blue) and with (red) the perturbation.

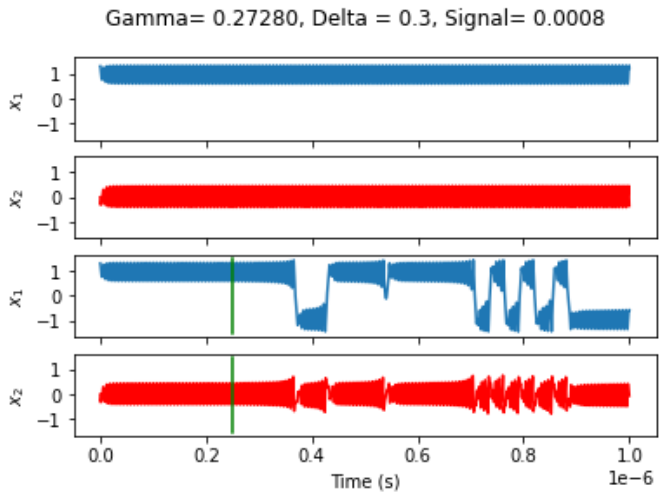

Fig. 12. Plot of the Duffing variables showing the transition from pseudo-periodic to chaotic, the defect occurs at 2.5 10^{-7}s (green line).

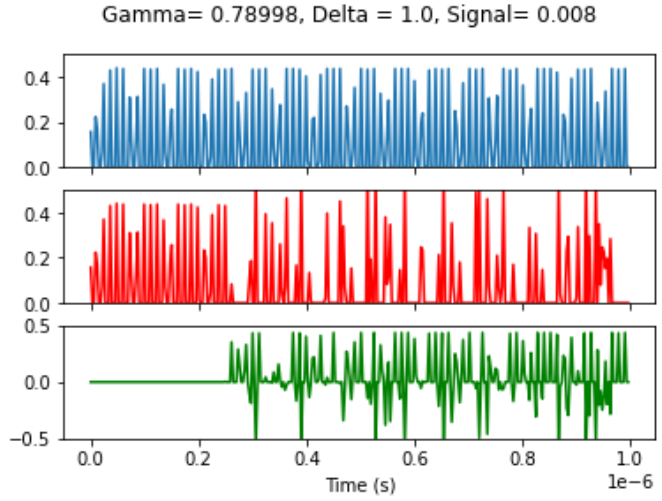

Fig. 13. Presence rate of the trajectory in the central zone, γ_c = 0.7899768... Upper curve: unperturbed oscillator, medium: oscillator with perturbation signal, lower: difference of the 2 curves.

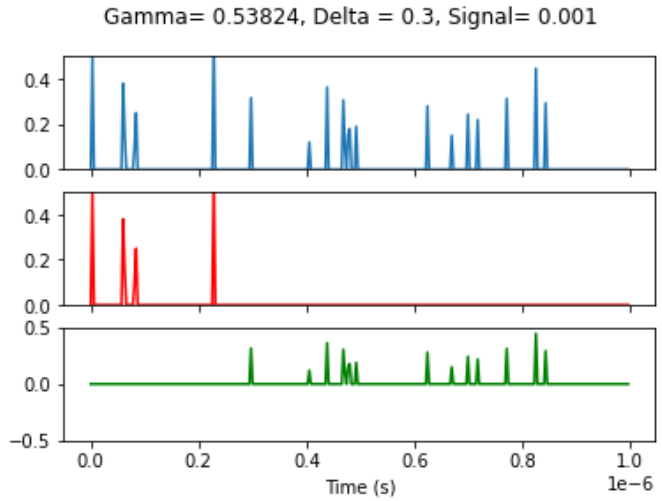

Fig. 14. Presence rate of the trajectory in the central zone, γ_c = 0.53824187... Upper curve: unperturbed oscillator, medium: oscillator with perturbation signal, lower: difference of the 2 curves.

in the central zone.

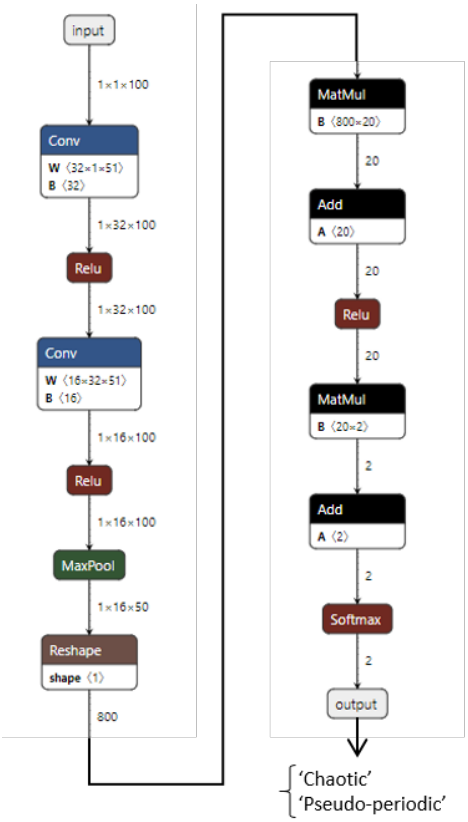

Fig. 15. Topology of a 1D convolutional neural network for transition detection.

V. Hardware Implementation

A possible implementation of the method is presented on Figure 16: the diagnosis system is made of an analog part and a digital part. The former generates a harmonic signal at a given frequency f (FDR generator) and injects it down the cable under test through a microwave circulator. The signal sent back by the cable is digitized and fed into the digital part of the system. This numeric data is added to a Duffing oscillator, as per equation (3), and the values of the state variables (x_1 and x_2) are analysed to detect a possible change of the behavior of the oscillator. Given the numerical precision required, this last part must be run on a computer capable of handling a precision of at least 32 bits.

Such a system can also run 2 oscillators in parallel: one with no perturbation as a reference, and the other with the additional signal from the cable. Comparing the values of the state variables of the two oscillators over time enables to detect a defect in the cable. However, as mentioned in the previous section, the values of the x_2 variable can be fed into a properly trained neural network to better detect and locate the defect.

As the system uses a monochromatic diagnosis signal, the design of the analog part remains quite simple, and a narrow band bandpass filter can be used after the circulator to reduce the noise introduced in the system.

Such a system can be used to detect the occurrence of a fault and trigger an alarm, or to locate a fault. In the first case, the probe signal is sent continuously into the cable and the change in state of the oscillator is an indication that a fault has occurred. In the second case, the signal is sent periodically through the cable and the oscillator is monitored afterwards. If the state of the oscillator has changed, the distance to the fault can be calculated using $D = \Delta t * c/2$ where Δt is the difference between the signal injection time and the oscillator state change time. The simulations in section IV have shown that the accuracy in the distance to the fault is of the order of magnitude of a metre, which means that this method should be used to diagnose long cables.

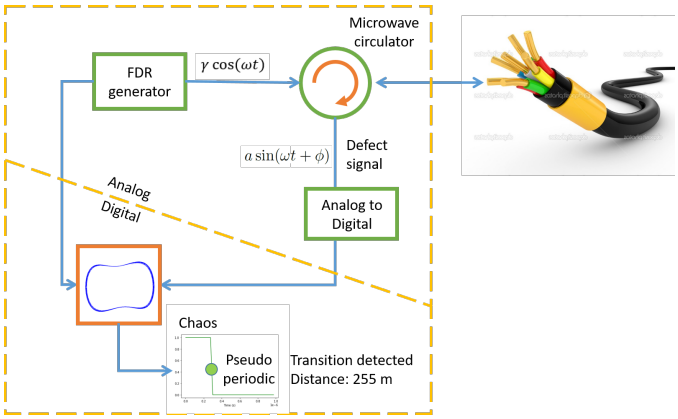

Fig. 16. Example of hardware implementation.

VI. Conclusion

This paper has presented the proof of concept of a new method, based on the frequency domain reflectometry (FDR), able to detect and locate incipient defects on long cables, thanks to chaotic analysis. Standard reflectometry methods rely on the analysis of echoes created by faults on the cable, but are limited when it comes to detecting incipient faults. The method proposed here does not analyse the signal returned by the cable but uses this signal to disturb a chaotic system previously set in an unstable equilibrium position. The use of a chaotic Duffing oscillator with critical parameters setting it near a chaotic transition provides a very high sensitivity to any perturbation. This enables the detection of incipient defects, characterized by electrical signatures much lower than attainable with state of the art methods.

When the FDR generator injects the signal into the cable, a standing wave is created in the cable, which is therefore placed in a stationary electrical state. This stationary state encompasses all phenomena that occur during signal propagation within the cable (due to any inhomogeneity, such as one or more faults, junctions, connectors, load, etc.). The case described in this article is the simplest possible, since we assume that the signal is completely absorbed at the end of the cable. The stationary wave present in the cable is only the sum of the injected wave and the wave reflected at the defect. In cases where the cable is not matched at the end, or where different junctions or sections are present and create several reflected signals, or if the cable is not homogeneous, the shape of the standing wave will be different, but this does

not change the fact that the cable positions itself and remains in a stationary state. However, determining this stationary state is more complex than is envisaged in this document. If we are able to characterize this stationary state (either by theoretical calculation or by measurement), we simply need to inject it into the second member of the equation (1) so that it is taken into account in the state equation of the chaotic oscillator. A frequency model able to compute the stationary wave present in a complex topology wired network with any kind of defect is provided in [29]. It requires the knowledge of the primary propagation parameters of the cable, the per unit length resistance, inductance, capacitance and conductance [30]. The updated equation will then be used to determine a set of critical parameters that will naturally take into account the presence of these cable artifacts. Any perturbation to this complex critical state can then be detected as before.

REFERENCES

[1] C. M. Furse, M. Kafal, R. Razzaghi, and Y.-J. Shin, "Fault Diagnosis for Electrical Systems and Power Networks: A Review," *IEEE Sensors Journal*, vol. 21, no. 2, pp. 888–906, 2021.

[2] G. Millet, S. Bruillot, D. Dejardin, N. Imbert, F. Auzanneau, L. Incarbone, M. Olivas, L. Vincent, A. Cremezi, and S. Poignant, "Aircraft Electrical Wiring Monitoring System," in *Embedded Real Time Software and Systems (ERTS2014)*, Toulouse, France, Feb. 2014. [Online]. Available: https://hal.science/hal-02272238

[3] F. Auzanneau, "Wire Troubleshooting and Diagnosis: Review and Perspectives," *Progress In Electromagnetics Research B*, vol. 49, pp. 253–279, 2013.

[4] N. K. Tumkur Jayakumar, M. U. Saleh, E. Benoit, J. Lacombe, M. Scarpulla, and C. Furse, "Fault Detection In PV Strings Using SSTDR," in *2018 USNC-URSI Radio Science Meeting (Joint with AP-S Symposium)*, 2018, pp. 9–10.

[5] Laurent Sommervogel, "Various Models for Faults in Transmission Lines and Their Detection Using Time Domain Reflectometry," *Progress In Electromagnetics Research C*, vol. 103, pp. 123–135, 2020.

[6] M. Kafal, F. Mustapha, W. Ben Hassen, and J. Benoit, "A Non Destructive Reflectometry Based Method for the Location and Characterization of Incipient Faults in Complex Unknown Wire Networks," in *2018 IEEE AUTOTESTCON*, 2018, pp. 1–8.

[7] W. B. Hassen and M. Kafal, "Shielding Damage Characterization in Twisted Pair Cables Using OMTDR-based Reflectometry and Inverse Problems," in *2019 PhotonIcs and Electromagnetics Research Symposium - Spring (PIERS-Spring)*, 2019, pp. 3093–3101.

[8] C. Furse, Y. C. Chung, R. Dangol, M. Nielsen, G. Mabey, and R. Woodward, "Frequency-domain reflectometry for on-board testing of aging aircraft wiring," *IEEE Transactions on Electromagnetic Compatibility*, vol. 45, no. 2, pp. 306–315, 2003.

[9] M. Kafal and W. B. Hassen, "On the Diagnosis of Incipient Faults in Transmission Lines Using a Projection Approach Based on Phase Patterns," in *2019 Photonics and Electromagnetics Research Symposium - Fall (PIERS - Fall)*, 2019, pp. 1288–1294.

[10] Y. H. Lee and Y.-J. Shin, "Time-Frequency Domain Reflectometry for Live HTS Cable System via Inductive Couplers and Neural Network," *IEEE Transactions on Applied Superconductivity*, vol. 31, no. 5, pp. 1–5, 2021.

[11] L. Abboud, A. Cozza, and L. Pichon, "A Noniterative Method for Locating Soft Faults in Complex Wire Networks," *IEEE Transactions on Vehicular Technology*, vol. 62, no. 3, pp. 1010–1019, 2013.

[12] M. Kafal, J. Benoit, A. Cozza, and L. Pichon, "A Statistical Study of DORT Method for Locating Soft Faults in Complex Wire Networks," *IEEE Transactions on Magnetics*, vol. 54, no. 3, pp. 1–4, 2018.

[13] H. Xu, J. Li, L. Liu, B. Wang, J. Zhang, and Y. Wang, "Chaos time domain reflectometry for fault location on live wires," *J. Appl. Anal. Comput*, vol. 5, no. 2, pp. 243–250, 2015.

[14] J. G. Zhang, H. Xu, B. J. Wang, L. Liu, P. C. Su, and J. X. Li, "Wiring fault detection with Boolean-chaos time-domain reflectometry," *Nonlinear Dynamics*, vol. 80, pp. 553–559, 2015, publisher: Springer.

[15] F. Auzanneau, "Chaos Time-domain Reflectometry For Distributed Diagnosis Of Complex Topology Wired Networks," *Electron. lett.*, vol. 52, no. 4, pp. 280–281, 2016.

[16] I. Bzikha, P. Monferran, V. Velayudhan, and A. Reineix, "Analysis of Chaos Time Domain Reflectometry for the Soft Fault Detection in a Cable," in *2020 International Symposium on Electromagnetic Compatibility-EMC EUROPE*. IEEE, 2020, pp. 1–6.

[17] F. Auzanneau, "Detection and Characterization of Microsecond Intermittent Faults in Wired Networks," *IEEE Transactions on Instrumentation and Measurement*, vol. 67, no. 9, pp. 2256–2258, 2018.

[18] ——, "Binary time domain reflectometry: a simpler and more efficient way of diagnosing defects in wired networks," in *2018 IEEE AUTOTESTCON*, 2018, pp. 1–8.

[19] ——, "Natural amplification of soft defects signatures in cables using binary time domain reflectometry," *IEEE Sensors Journal*, vol. 21, no. 2, pp. 937–944, 2019, publisher: IEEE.

[20] A. Cozza, "Never Trust a Cable Bearing Echoes: Understanding Ambiguities in Time-Domain Reflectometry Applied to Soft Faults in Cables," *IEEE Transactions on Electromagnetic Compatibility*, vol. 61, no. 2, pp. 586–589, 2019.

[21] D. Chen, S. Shi, X. Gu, and B. Shim, "Weak Signal Frequency Detection Using Chaos Theory: A Comprehensive Analysis," *IEEE Transactions on Vehicular Technology*, vol. 70, no. 9, pp. 8950–8963, 2021.

[22] X. Xiang and B. Shi, "Weak signal detection based on the information fusion and chaotic oscillator," *Chaos: An Interdisciplinary Journal of Nonlinear Science*, vol. 20, no. 1, 2010, publisher: AIP Publishing.

[23] G. Duffing, *Erzwungene schwingungen bei veränderlicher eigenfrequenz und ihre technische bedeutung*, ser. Sammlung Vieweg. F. Vieweg & Sohn, 1918. [Online]. Available: https://books.google.fr/books?id=s3W4AAAAIAAJ

[24] W. Wei, L. Qiang, and Z. Guojie, "Novel approach based on chaotic oscillator for machinery fault diagnosis," *Measurement*, vol. 41, no. 8, pp. 904–911, 2008. [Online]. Available: https://www.sciencedirect.com/science/article/pii/S0263224108000079

[25] Z. Zhihong and Y. Shaopu, "Application of Van de Pol - Duffing oscillator in weak signal detection," *Computer and electrical engineering*, vol. 41, pp. 1–8, 2015.

[26] G. Wang, D. Chen, J. Lin, and X. Chen, "The application of chaotic oscillators to weak signal detection," *IEEE Transactions on Industrial Electronics*, vol. 46, no. 2, pp. 440–444, 1999.

[27] A. Dabrowski, T. Sagan, V. Denysenko, M. Balcerzak, S. Zarychta, and A. Stefanski, "Alternative Methods of the Largest Lyapunov Exponent Estimation with Applications to the Stability Analyses Based on the Dynamical Maps - Introduction to the Method," *Materials*, vol. 14, no. 23, 2021.

[28] M. Kafal and J. Benoit, "Baselining: A Critical Approach Used for Soft Fault Detection in Wire Networks," *International Journal of Digital Information and Wireless Communications*, vol. 8, no. 1, 2018.

[29] F. Auzanneau and N. Ravot, "Détection et localisation de défauts dans des réseaux filaires de topologie complexe," *Annales Des Télécommunications*, vol. 62, no. 1, pp. 193–213, Jan. 2007. [Online]. Available: https://doi.org/10.1007/BF03253256

[30] N. Idir, Y. Weens, and J.-J. Franchaud, "Skin effect and dielectric loss models of power cables," *IEEE Transactions on Dielectrics and Electrical Insulation*, vol. 16, no. 1, pp. 147–154, 2009.

Fabrice Auzanneau graduated from Ecole Nationale Supérieure de l'Aéronautique et de l'Espace (now ISAE) in 1987 and began to work at CEA (French Atomic Energy Commission) in 1988 as a research engineer on electromagnetic stealth problems. He worked one year in 1997 at the University of Arizona, Tucson, as a visiting scholar studying artificial metamaterials. He then became assistant to the Director of CEA DAM in 1998. In 2001, he joined CEA Technological Research Division and became the head of the Laboratory for the Reliability of Embedded Systems in 2003. He was then deputy director of the Architecture and Embedded Software Division of CEA and is now researcher in the Embedded Artificial Intelligence Laboratory of CEA List. His research interests concern metamaterials, wire diagnosis methods and tools, and AI.